Parquet-graph resummation method for vortex liquids

Joonhyun Yeo and M. A. Moore
Department of Physics, University of Manchester, Manchester M13 9PL, United Kingdom
(Received 13 March 1996)

We present in detail a nonperturbative method for vortex liquid systems. This method is based on the resummation of an infinite subset of Feynman diagrams, the so-called parquet graphs, contributing to the four-point vertex function of the Ginzburg-Landau model for a superconductor in a magnetic field. We derive a set of coupled integral equations, the parquet equations, governing the structure factor of the two-dimensional vortex liquid system with and without random impurities and the three-dimensional system in the absence of disorder. For the pure two-dimensional system, we simplify the parquet equations considerably and obtain one simple equation for the structure factor. In two dimensions, we solve the parquet equations numerically and find growing translational order characterized by a length scale R_c as the temperature is lowered. The temperature dependence of R_c is obtained in both pure and weakly disordered cases. The effect of disorder appears as a smooth decrease of R_c as the strength of disorder increases. [S0163-1829(96)02729-4]

I. INTRODUCTION

Since the discovery of high-T_c superconductors, the nature of the mixed state in a type-II superconductor has been a focus of theoretical and experimental investigation. In many high-T_c materials, thermal fluctuations are responsible for the melting of the vortex lattice phase predicted by the mean-field theory[1] into a vortex liquid phase. The presence of quenched random impurities in the vortex liquid or lattice phases also plays an important role, since it presents a possibility of a dissipation-free current flow due to pinning of flux lines. Theoretical phases such as the vortex glass phase[2] for point defects and the Bose glass phase[3] in the presence of extended defects have been proposed. As shown by Larkin and Ovchinnikov[4] (LO) the quenched point disorder destroys, for spatial dimension $d<4$, the long-range crystalline order of the vortex lattice. The system is described by some characteristic length scale R_c over which a short-range translational order exists.

In a previous paper,[5] we developed a nonperturbative scheme to calculate the structure factor of the two-dimensional (2D) vortex liquid in the absence of random impurities. The main ingredient of this nonperturbative method was the resummation of an infinite subset of Feynman diagrams contributing to the structure factor, the so-called parquet graphs.[6] This is an analytic approach to the 2D vortex liquid system which is sophisticated enough to predict growing crystalline order in the system as the temperature is lowered. The growth of the translational order was investigated in connection with the sharp peaks developing in the liquid structure factor. Within this scheme, we found no evidence for a finite temperature phase transition into the vortex lattice phase and the system remains as a liquid. The length scale R_c, characterizing this growing translational order, seemed to diverge only in the zero-temperature limit.

In this paper, we give detailed derivations of the parquet-graph resummation technique which were omitted in the previous paper.[5] In addition, we present a simplified version of the parquet equations governing the structure factor, which were given in terms of a set of *coupled* nonlinear integral equations previously. In the present work, we were able to obtain one simple equation for the structure factor, which contains all the nonperturbative information for the 2D vortex liquid in the absence of disorder.

In this paper, we also apply the parquet-graph resummation technique to the 2D vortex liquid in the presence of quenched disorder. We find that the sharp peaks which appeared in the structure factor of the pure system become broadened as the strength of the disorder increases. This is entirely consistent with one's intuition that in the presence of disorder the length scale R_c describing the translational order becomes smaller as compared to the pure case. In the present work, since our pure system is always in the liquid phase, the effect of disorder appears as smooth deviations from the pure case. From the nonperturbative results, we find the temperature dependence of the length scale R_c. It is, however, difficult to make any connection between our results and the LO-type argument, since there exists no vortex lattice phase at any finite temperature within our nonperturbative scheme, while the LO argument always starts from the vortex lattice with a true long-range crystalline order.

We note that there exist recent theoretical studies[7] based on the elastic theory of pinned lattices suggesting that the pinning by quenched disorder becomes less effective due to the periodicity of the lattice so that a quasi-long-range order persists beyond the Larkin length scale R_c. In the present nonperturbative analysis, the existence of such quasi-long-range translational order has not been observed.

The point whether the 2D vortex liquid in the absence of disorder undergoes a finite-temperature phase transition into a 2D vortex lattice is still controversial. Numerical simulations[8] seem to suggest a first-order phase transition. However, as shown in Ref. 9, these results depend crucially on boundary conditions. In a spherical geometry, the authors of Ref. 9 demonstrated the absence of a finite-temperature phase transition. There also exists a recent experiment[10] performed on a sample with very weak pinning, where no sign of a phase transition is detected. The present parquet approximation, which is an analytic theory on an infinite plane, seems to support the absence of a finite temperature phase

transition between 2D vortex liquid and solid.

Unlike the 2D system, it is generally believed that a 3D vortex liquid undergoes a first-order phase transition into a vortex lattice. An experiment by Zeldov *et al.*[11] on Bi-Sr-Ca-Cu-O has been accepted as convincing evidence for the transition. However, there exists a recent claim[12] that the results of Ref. 11 might be an artifact due to a particular sample geometry. Therefore, it would be interesting if one could develop a three-dimensional parquet-graph resummation scheme and obtain nonperturbative information on the 3D vortex liquid system. We find that one can generalize the parquet equations to three dimensions without difficulty. Unfortunately, the equations become very complicated and we were not able to obtain a numerical solution to the 3D parquet equations.

In the next section, we introduce the structure factor of a two-dimensional disordered vortex liquid within the Ginzburg-Landau theory. In Secs. III and IV, we present detailed derivations of the parquet equations which account for all the parquet graphs contributing to the structure factor for both pure and disordered cases. We also consider zero-dimensional models to discuss the validity of the parquet approximation in general. In the following section, we present the main results of our calculation and discuss the temperature dependence of the length scale R_c. In Sec. VI, we present the generalization of the parquet equations to three dimensions. Finally, we conclude with a discussion on future directions.

II. THE STRUCTURE FACTOR

We begin our analysis with the Ginzburg-Landau (GL) free energy for a superconducting film in a perpendicular magnetic field $\mathbf{B}=\boldsymbol{\nabla}\times\mathbf{A}$ in the presence of quenched random impurities,

$$F[\Psi]=\int d^2\mathbf{r}\left(\frac{1}{2m}|(-i\hbar\boldsymbol{\nabla}-e^*\mathbf{A})\Psi|^2+[\alpha+\tau(\mathbf{r})]|\Psi|^2+\frac{\beta}{2}|\Psi|^4\right), \tag{2.1}$$

where α, β, and m are phenomenological parameters. The random field $\tau(\mathbf{r})$ representing the quenched impurities satisfies the probability distribution, $\overline{\tau(\mathbf{r})}=0$ and

$$\overline{\tau(\mathbf{r})\tau(\mathbf{r}')}=\lambda\delta^{(2)}(\mathbf{r}-\mathbf{r}'). \tag{2.2}$$

In this paper we neglect the fluctuations in the vector potential $\mathbf{A}$ and restrict the order parameter Ψ to the space spanned by the lowest-Landau-level (LLL) wave functions. In the symmetric gauge, where $\mathbf{A}=(B/2)(-y,x)$, the LLL is fully described by an arbitrary analytic function of the variable $z=x+iy$ multiplied by an exponential factor; $\Psi(x,y)=\exp(-(\mu^2/4)z^*z)\phi(z)$, where $\mu^2\equiv e^*B/\hbar=2\pi/Q$ and Q is the area of the unit cell of the vortex lattice. In the LLL approximation, the GL free energy becomes

$$F[\phi]=\int dz^*dz\left[[\alpha_H+\tau(z,z^*)]\exp\left(-\frac{\mu^2}{2}|z|^2\right)|\phi(z)|^2+\frac{\beta}{2}\exp(-\mu^2|z|^2)|\phi(z)|^4\right], \tag{2.3}$$

where $\int dz^*dz$ denotes the integration over the x-y plane and $\alpha_H\equiv\alpha+\hbar e^*B/2m$ vanishes at the mean-field transition temperature.

The central quantity in this analysis is the structure factor of the two-dimensional vortex liquid. It is proportional to the Fourier transform of the density-density correlation function, $\tilde{\chi}(\mathbf{k})=\int d^2\mathbf{R}e^{i\mathbf{k}\cdot\mathbf{R}}\chi(\mathbf{r},\mathbf{r}+\mathbf{R})$,

$$\chi(\mathbf{r},\mathbf{r}')\equiv\overline{\langle|\Psi(\mathbf{r})|^2|\Psi(\mathbf{r}')|^2\rangle}-\overline{\langle|\Psi(\mathbf{r})|^2\rangle}\;\overline{\langle|\Psi(\mathbf{r}')|^2\rangle},$$

where the angular brackets denote the thermal averages. The structure factor $\Delta(\mathbf{k})$ is then defined by

$$Q\exp\left(-\frac{\mathbf{k}^2}{2\mu^2}\right)\Delta(\mathbf{k})\equiv\tilde{\chi}(\mathbf{k})/[\overline{\langle|\Psi(\mathbf{r})|^2\rangle}]^2. \tag{2.4}$$

A convenient way to deal with quenched averages is to introduce n replicas of Z and calculate the correlation functions with respect to

$$\overline{Z^n}=\int\prod_a^n d\phi_a^*d\phi_a\exp\left[-\int dz^*dz\left\{\alpha_He^{-\mu^2|z|^2/2}\times\sum_a|\phi_a(z)|^2+\frac{\beta}{2}e^{-\mu^2|z|^2}\sum_a|\phi_a(z)|^4-\frac{\lambda}{2}e^{-\mu^2|z|^2}\sum_{a,b}|\phi_a(z)|^2|\phi_b(z)|^2\right\}\right] \tag{2.5}$$

in the limit $n\to0$. One can develop a standard perturbation theory for (2.5). The bare propagator arising from the perturbation expansion of (2.5) is given by[13]

$$G_0^{ab}(\zeta^*,z)\equiv\langle\langle\phi_a^*(\zeta^*)\phi_b(z)\rangle\rangle_0=\delta_{ab}\frac{1}{\alpha_H}\frac{\mu^2}{2\pi}\exp\left(\frac{\mu^2}{2}\zeta^*z\right), \tag{2.6}$$

where the double bracket $\langle\langle\cdots\rangle\rangle$ denotes the average with respect to $\overline{Z^n}$. It is important to note that, because of the simple quadratic term of the LLL free energy in (2.5), the renormalized propagator G_R^{ab} is obtained by simply replacing α_H by the renormalized mass α_R. This means that the magnetic length μ^{-1} is the only length scale involved in the renormalized propagator. This is one of the simplifying features of the LLL approximation that makes the present nonperturbative calculation feasible.

As noticed in Ref. 13, the GL free energy obtained from (2.5) is not closed under renormalization. The renormalization effectively generates the quartic vertices of a general form,

$$\int \prod_{i=1,2} dz_i^* dz_i e^{-(\mu^2/2)(|z_1|^2+|z_2|^2)} \Bigg[\sum_{a,b} |\phi_a(z_1)|^2 \times (\delta_{ab} g(|z_1-z_2|) - w(|z_1-z_2|)) |\phi_b(z_2)|^2 \Bigg], \tag{2.7}$$

for arbitrary functions g and w. The bare interactions correspond to

$$g_B(|z|) = \frac{\beta}{2}\delta(z)\delta(z^*), \quad w_B(|z|) = \frac{\lambda}{2}\delta(z)\delta(z^*).$$

It is convenient to work with the Fourier transform[14]

$$\tilde{g}(\mathbf{k}) = \int dz^* dz g(|z|) \exp\left(\frac{i}{2}(k^* z + k z^*)\right)$$

and similarly $\tilde{w}(\mathbf{k})$, where k, k^* are complex momenta, $k = k_1 + ik_2, k^* = k_1 - ik_2$ with $\mathbf{k} = (k_1, k_2)$. Thus, $\tilde{g}_B(|k|) = \beta/2$ and $\tilde{w}_B(|k|) = \lambda/2$ are constants.

In order to calculate the structure factor, (2.4), we need to consider the renormalized four-point correlation function arising from Eq. (2.5),

$$\langle\langle \phi_a^*(z_1^*)\phi_b^*(z_2^*)\phi_c(z_3)\phi_d(z_4)\rangle\rangle = G_R^{ac}(z_1^*, z_3) G_R^{bd}(z_2^*, z_4) + G_R^{bc}(z_2^*, z_3) G_R^{ad}(z_1^*, z_4) + \langle\langle \phi_a^*(z_1^*)\phi_b^*(z_2^*)\phi_c(z_3)\phi_d(z_4)\rangle\rangle_c,$$

where the last term denotes the contribution from all connected Feynman diagrams. To the lowest order of perturbation theory, the connected four-point correlation function can easily be calculated as

$$\langle\langle \phi_a^*(z_1^*)\phi_b^*(z_2^*)\phi_c(z_3)\phi_d(z_4)\rangle\rangle_c = -\delta_{ac}\delta_{bd}\frac{2}{\alpha_R^4}\left(\frac{\mu^2}{2\pi}\right)^2 e^{\mu^2(z_1^* z_3 + z_2^* z_4)/2} \int \frac{dk^* dk}{(2\pi)^2} [\delta_{ab}\tilde{g}_B(|k|) - \tilde{w}_B(|k|)] e^{-|k|^2/\mu^2} e^{-i[k^*(z_3 - z_4) + k(z_1^* - z_2^*)]/2} + (c \leftrightarrow d, z_3 \leftrightarrow z_4) + O(\beta^2, \beta\lambda, \lambda^2), \tag{2.8}$$

where the second term on the right-hand side is the same as the first term with c and d, and z_3 and z_4 interchanged. In (2.8), we absorbed the renormalization of the propagators using the renormalized mass α_R. To the lowest order, one can easily evaluate the $\mathbf{k}$ integrals in (2.8), but, in general, higher-order corrections to the connected four-point function are represented in (2.8) by the departure of the quartic vertex functions from constants, $\tilde{g}_B(|k|) = \beta/2$ and $\tilde{w}_B(|k|) = \lambda/2$, to general $\mathbf{k}$-dependent functions, $\tilde{g}_R(\mathbf{k})$ and $\tilde{w}_R(\mathbf{k})$. Therefore, the LLL approximation enables us to concentrate on the renormalized quartic vertex functions $\tilde{g}_R(\mathbf{k})$ and $\tilde{w}_R(\mathbf{k})$, which depend only on one variable instead of three characterizing three independent channels in a usual field theory.

Now, one can put (2.8) for general $g_R(\mathbf{k})$ and $w_R(\mathbf{k})$ in a more symmetric form using scaled functions,

$$f_R(\mathbf{k}) \equiv \frac{2}{\beta}\exp(-\mathbf{k}^2/2\mu^2)\tilde{g}_R(\mathbf{k}),$$

$$v_R(\mathbf{k}) \equiv \frac{2}{\lambda}\exp(-\mathbf{k}^2/2\mu^2)\tilde{w}_R(\mathbf{k}).$$

The bare vertices are given by $f_B(k) = v_B(k) = \exp(-\mathbf{k}^2/2\mu^2)$. Interchanging z_3 and z_4 in the second term on the right-hand side of (2.8) is equivalent to using, instead of $f_R(\mathbf{k})$ and $v_R(\mathbf{k})$, the transformed functions, $\hat{f}_R(\mathbf{k})$ and $\hat{w}_R(\mathbf{k})$, where $\hat{f}(\mathbf{k})$ is defined for an arbitrary function $f(\mathbf{k})$ by[15]

$$\hat{f}(\mathbf{k}) \equiv \frac{2\pi}{\mu^2}\int \frac{d^2\mathbf{p}}{(2\pi)^2} f(\mathbf{p}) \exp\left(\frac{i}{\mu^2}(k_1 p_2 - k_2 p_1)\right),$$

$$f(\mathbf{k}) = \frac{2\pi}{\mu^2}\int \frac{d^2\mathbf{p}}{(2\pi)^2} \hat{f}(\mathbf{p}) \exp\left(\frac{i}{\mu^2}(k_1 p_2 - k_2 p_1)\right).$$

The general four-point function is then given by (see the Appendix)

$$\langle\langle \phi_a^*(z_1^*)\phi_b^*(z_2^*)\phi_c(z_3)\phi_d(z_4)\rangle\rangle_c = -\frac{4}{\alpha_R^4}\left(\frac{\mu^2}{2\pi}\right)^2 \exp\left(\frac{\mu^2}{2}(z_1^* z_3 + z_2^* z_4)\right) \times \int \frac{dk^* dk}{(2\pi)^2}\frac{\beta}{2}\Gamma_{ab,cd}(\mathbf{k}) \exp\left(-\frac{|k|^2}{2\mu^2} - \frac{i}{2}[k^*(z_3 - z_4) + k(z_1^* - z_2^*)]\right), \tag{2.9}$$

where

$$\Gamma_{ab,cd}(\mathbf{k}) = \frac{1}{2}\delta_{ac}\delta_{bd}[\delta_{ab} f_R(\mathbf{k}) - \theta v_R(\mathbf{k})] + \frac{1}{2}\delta_{ad}\delta_{bc}[\delta_{ab}\hat{f}_R(\mathbf{k}) - \theta\hat{v}_R(\mathbf{k})], \tag{2.10}$$

and $\theta \equiv \lambda/\beta$ represents the strength of the disorder. Equation (2.10) can be represented diagrammatically as in Fig. 1.

The structure factor $\Delta(\mathbf{k})$ is then obtained by joining two external legs of the four-point correlation functions, (2.9). From (2.9) and (2.10) and the definition (2.4) in the limit $n \to 0$, we obtain

$$\Delta(\mathbf{k}) = 1 - 2x\Gamma(\mathbf{k}), \tag{2.11}$$

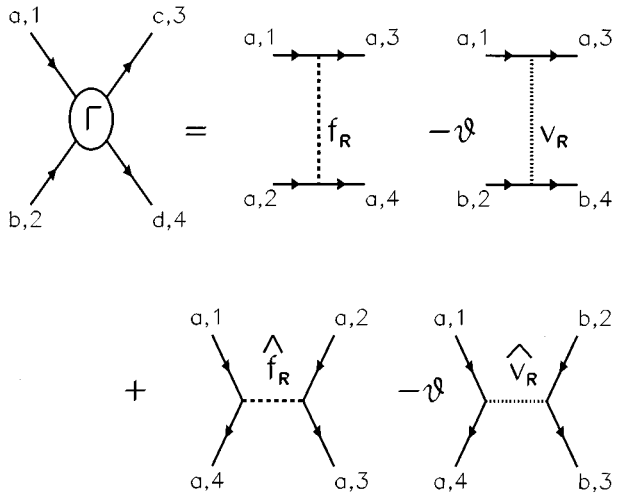

FIG. 1. Diagrammatic representation of the renormalized connected four-point correlation function. The labels, 1, . . . ,4, denote z_1^*, z_2^*, z_3, z_4, respectively, and $a, \ldots, d$ are replica indices.

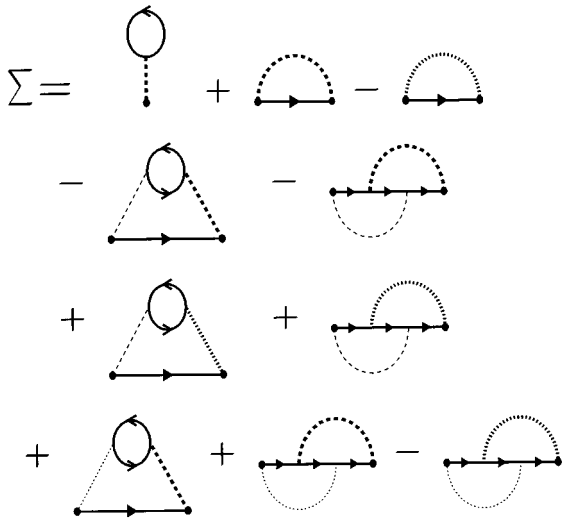

FIG. 2. Diagrammatic representation of Dyson equation for the self-energy Σ. The solid lines represent the renormalized propagators. The thick dashed and dotted lines are the renormalized vertex functions, f_R and v_R, as in Fig. 1, while the thin dashed and dotted lines denote the bare vertex functions, f_B and v_B, respectively.

where

$$\Gamma(\mathbf{k}) \equiv \frac{1}{2}\{f_R(\mathbf{k}) + \hat{f}_R(\mathbf{k}) - \theta[v_R(\mathbf{k}) + \hat{v}_R(\mathbf{k})]\} \quad (2.12)$$

and $x \equiv \mu^2\beta/2\pi\alpha_R^2$ is a dimensionless parameter which appears in the high-temperature perturbation expansion.[16,17]

In the following sections, we will evaluate $f_R(\mathbf{k})$ and $v_R(\mathbf{k})$ nonperturbatively by summing the parquet graphs. As mentioned earlier, we absorb any renormalization of the propagator into the renormalized parameter α_R. But knowledge of the four-point vertex function also fixes the relationship between α_R and the bare parameter α_H, thus completing the description of the system. This relation comes from the Dyson equation arising from (2.5) which is described diagrammatically in Fig. 2 for the self-energy $\Sigma = G^{-1} - G_0^{-1} = 2\pi(\alpha_R - \alpha_H)/\mu^2$:

$$\alpha_T = \frac{1}{\sqrt{x}}\left[1 - x(2-\theta) + x^2\frac{2\pi}{\mu^2}\int \frac{d^2\mathbf{k}}{(2\pi)^2} e^{-k^2/2\mu^2} \times [2(1-\theta)f_R(\mathbf{k}) - \theta(2-\theta)v_R(\mathbf{k})]\right], \quad (2.13)$$

where $\alpha_T \equiv \alpha_H\sqrt{2\pi/\beta\mu^2}$ is the dimensionless temperature. Note that this is an *exact* relationship between the renormalized propagator and the quartic vertex functions. We will, however, use $f_R(\mathbf{k})$ and $v_R(\mathbf{k})$ obtained from the present nonperturbative approximation. The Hartree approximation used in the high-temperature perturbation expansion[16] corresponds to neglecting terms that depend on the vertex functions, f_R and v_R.

III. PARQUET-GRAPH RESUMMATION: PURE SYSTEM ($\lambda = 0$)

In order to calculate $f_R(\mathbf{k})$ and $v_R(\mathbf{k})$, one needs to evaluate the Feynman diagrams contributing to the four-point correlation function. In this and the next section, we show in detail how to sum an infinite subset of such diagrams, the so-called parquet graphs.

We first consider the pure system where $\lambda = 0$, then generalize the result to the disordered case. The analysis of the pure case will mostly reproduce results given in Ref. 5. In the present work, we make a further simplification of the parquet equation for $f_R(\mathbf{k})$ found in Ref. 5 and obtain a very simple equation for the structure factor $\Delta(\mathbf{k})$.

For both pure and disordered cases, we will present the analysis for the zero-dimensional analogs of (2.3), which can be integrated exactly. For the pure case, we find it convenient to introduce the parquet resummation scheme in a simple zero-dimensional model and then generalize to the two-dimensional problem. Furthermore, since there is no apparent expansion parameter involved in the parquet approximation, it would be instructive to apply the parquet resummation to the cases where exact solutions are known and to compare the approximate result with the exact solution.

A. $d = 0$

For $\lambda = 0$ and dimension $d = 0$, the partition function corresponding to (2.3) is a simple integral,

$$Z(\alpha_H, \beta) = \int \frac{d\psi d\psi^*}{2\pi} \exp\left(-\alpha_H|\psi|^2 - \frac{\beta}{2}|\psi|^4\right) = \sqrt{\frac{\pi}{2\beta}}\,\mathrm{erfc}(\sigma)\exp(\sigma^2),$$

where $\sigma = \alpha_H/\sqrt{2\beta}$ and $\mathrm{erfc}(\sigma) \equiv 1 - \mathrm{erf}(\sigma)$ is the complementary error function. In the parquet analysis, one calculates the renormalized four-point vertex

$$\Gamma \equiv -\frac{\alpha_R^4}{4}\langle|\psi|^4\rangle_c = \frac{\alpha_R^4}{2}\left[\frac{\partial}{\partial\beta}\ln Z + \frac{1}{\alpha_R^2}\right],$$

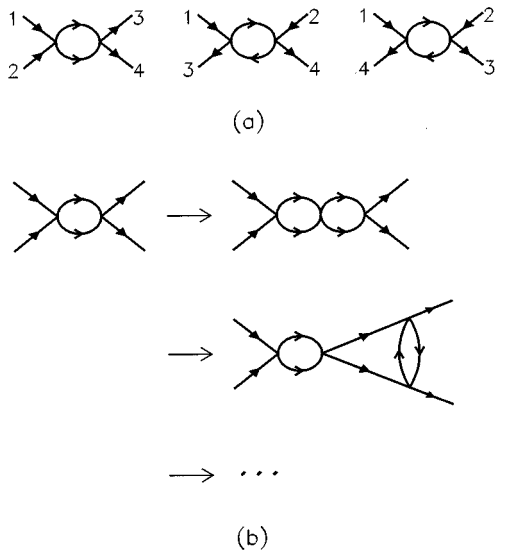

FIG. 3. (a) Three one-loop diagrams. The symmetry factors are 2, 4, and 4, respectively. The labels $1,\ldots,4$ are drawn for the general cases to be discussed later. For the zero-dimensional case, there is no distinction between the second and the third diagrams. But, it is important to separate this contribution into two equal parts. (b) An example of constructing successive parquet graphs.

where $\alpha_R^{-1}=\langle|\psi|^2\rangle$. Although an exact solution can readily be found, one can construct the usual Feynman graph expansion for Γ. To the lowest order, we have $\Gamma=\Gamma_B=\beta/2$. To the one-loop order, the diagrams can be represented as shown in Fig. 3. A convenient way to generate the next order diagrams is to replace each vertex in a one-loop diagram by the vertices obtained up to the one-loop order. In general, one can construct higher-order diagrams by replacing each vertex in the one-loop diagrams by the vertices obtained up to the current order of perturbation expansion. An example of such construction is shown in Fig. 3. The diagrams obtained in this way are called *parquet* graphs. Note that parquet graphs can be separated into two parts by cutting two propagator lines.

Although parquet graphs cover an enormous number of diagrams, obviously not all diagrams can be constructed in this way. The nonparquet diagrams are generated in the above construction by the so-called totally irreducible vertices whose contribution here is denoted by R. The totally irreducible vertex consists of the bare vertex and higher-order $[O(\beta^4)]$ vertices (see Fig. 4). There is no systematic way of enumerating these higher-order diagrams contributing to R. The parquet approximation which we employ in this work corresponds to keeping only the bare vertex contribution in R: $R\simeq\Gamma_B=\beta/2$ in the zero-dimensional case.

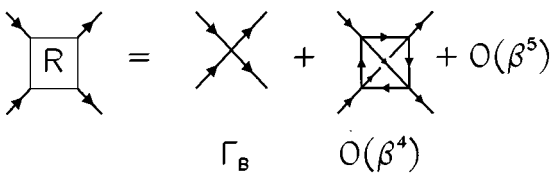

FIG. 4. The totally irreducible vertex R.

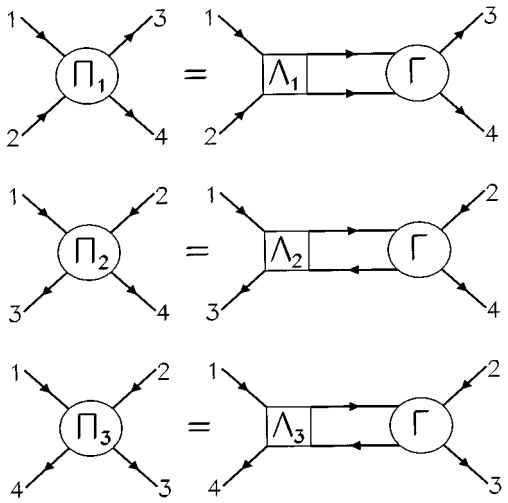

FIG. 5. The parquet decomposition of the reducible vertex Π_i. Again, the labels $1,\ldots,4$ are drawn for the general cases. The same diagrammatic decomposition can be used in higher dimensional models for both pure and disordered cases.

If *both* bare vertices in a one-loop diagram are replaced by the full renormalized vertex in the above construction of graphs, then the diagrams become overcounted. There is a systematic way to eliminate this overcounting and to generate all the Feynman diagrams and the symmetry factors associated with each diagram, and that is to use the full vertex for the bare vertex on the right-hand side of Fig. 3, but the so-called *irreducible* vertex for the one on the left-hand side, which is defined as follows: Let Π_i, $i=1,2,3$ denote the diagrams constructed out of the three one-loop diagrams in Fig. 3 and Λ_i the corresponding irreducible vertices, we have from Fig. 5

$$\Pi_1=-\frac{2}{\alpha_R^2}\Lambda_1\Gamma, \tag{3.1a}$$

$$\Pi_2=-\frac{4}{\alpha_R^2}\Lambda_2\Gamma, \tag{3.1b}$$

$$\Pi_3=-\frac{4}{\alpha_R^2}\Lambda_3\Gamma, \tag{3.1c}$$

where we absorb any renormalization on propagator lines into α_R. Now, for the irreducible vertex Λ_i, we must include all the diagrams that do not belong to Π_i to avoid the overcounting, thus, $\Lambda_i=\Gamma-\Pi_i$. Finally, the renormalized vertex Γ is given by the sum of all contributions:

$$\Gamma=R+\sum_{i=1}^{3}\Pi_i. \tag{3.2}$$

Therefore,

$$\Lambda_i=R+\sum_{j\neq i}\Pi_j. \tag{3.3}$$

Note that (3.1)–(3.3) are *exact* relations for the renormalized vertex Γ. But, as mentioned before, we use $R\simeq\beta/2$. To see

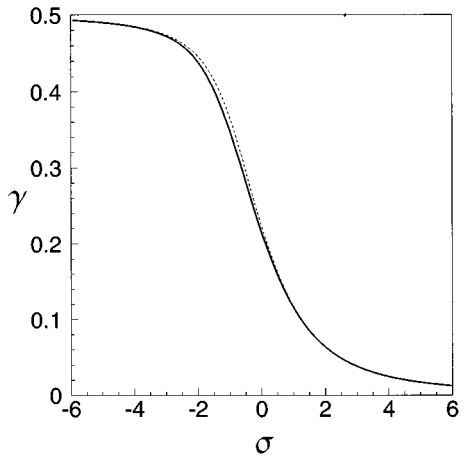

FIG. 6. The renormalized four-point vertex function γ for the pure zero-dimensional model as a function of temperature σ. The solid line is the exact solution. The dashed line corresponds to the parquet approximation.

which diagrams are explicitly summed by the parquet approximation, one iterates (3.1)–(3.3) starting with $R=\beta/2$. A listing of all parquet diagrams up to $O(\beta^6)$ is given in the review of Jackson *et al.*[6] (their Fig. 8, but their diagrammatic formalism is not identical to ours and we have additional diagrams to theirs since there are arrows on our propagators). In the language employed in many-body physics, within the parquet approach, all reducible two-particle diagrams are summed up by choosing an irreducible kernel (for us, the bare vertex) and by preserving the crossing symmetry of the four-point correlation function.

One can easily simplify the above equations for $R=\beta/2$ as follows: From (3.1), one has

$$\Pi_1=\frac{2\Gamma^2}{\alpha_R^2-2\Gamma}, \quad \Pi_2=\Pi_3=\frac{4\Gamma^2}{\alpha_R^2-4\Gamma}.$$

Therefore, from (3.2), we obtain

$$\gamma=\rho-\frac{\gamma^2}{1-\gamma}-2\frac{2\gamma^2}{1-2\gamma}, \tag{3.4}$$

where $\gamma\equiv 2\Gamma/\alpha_R^2$ and $\rho\equiv\beta/\alpha_R^2$. As a function of ρ, there is only one solution $\gamma(\rho)$ that satisfies the trivial condition: $\Gamma=\gamma=0$ when $\beta=\rho=0$.

To complete the description of the system, one needs a relation between the bare (α_H or σ) and renormalized (α_R or ρ) mass. In the parquet approximation, we use an analog of the Dyson equation, (2.13), which, in this case, is

$$\sigma=\frac{1}{\sqrt{2\rho}}[1-2\rho(1-\gamma)]. \tag{3.5}$$

From this relation using $\gamma=\gamma(\rho)$ obtained from (3.4), one finds ρ as a function of σ, and consequently we have the renormalized four-point vertex γ as a function of σ. In Fig. 6, $\gamma(\sigma)$ of the parquet approximation is compared with the exact solution. One can see there is excellent agreement between the two.

B. $d=2$

We now consider the two-dimensional problem in the absence of disorder. The parquet equations can be constructed similarly to the $d=0$ case. In fact, Eqs. (3.1)–(3.3) take almost the same form as before. The only differences are the fact that the vertices now depend on the internal momentum $\mathbf{k}$ and the right-hand sides of (3.1) should be obtained from a direct evaluation of diagrams in Fig. 5. In the Appendix, we show explicitly how this calculation is done. The resulting equations corresponding to (3.1) are

$$\Pi_1(\mathbf{k})=-x(\Lambda_1\circ\Gamma)(\mathbf{k}), \tag{3.6a}$$

$$\Pi_2(\mathbf{k})=-2x\Lambda_2(\mathbf{k})\Gamma(\mathbf{k}), \tag{3.6b}$$

$$\Pi_3(\mathbf{k})=-2x(\Lambda_3*\Gamma)(\mathbf{k}), \tag{3.6c}$$

where the operations $\circ$ and $*$ between two arbitrary functions $f(\mathbf{k})$ and $g(\mathbf{k})$ are defined by

$$(f\circ g)(\mathbf{k})\equiv\frac{2\pi}{\mu^2}\int\frac{d^2\mathbf{p}}{(2\pi)^2}f(\mathbf{k}-\mathbf{p})g(\mathbf{p})\cos\left(\frac{k_1p_2-k_2p_1}{\mu^2}\right),$$

$$(f*g)(\mathbf{k})\equiv\frac{2\pi}{\mu^2}\int\frac{d^2\mathbf{p}}{(2\pi)^2}f(\mathbf{k}-\mathbf{p})g(\mathbf{p}).$$

The remaining parquet equations are given by

$$\Gamma(\mathbf{k})=R(\mathbf{k})+\sum_{i=1}^{3}\Pi_i(\mathbf{k}), \tag{3.7}$$

$$\Lambda_i(\mathbf{k})=R(\mathbf{k})+\sum_{j\neq i}\Pi_j(\mathbf{k}), \tag{3.8}$$

where $R(\mathbf{k})$ represents the totally irreducible part. In the parquet approximation, $R(\mathbf{k})$ is equal to the bare vertex part: $R(\mathbf{k})\simeq(1/2)(f_B+\hat{f}_B)=\exp(-\mathbf{k}^2/2\mu^2)$.

We can make a simplification on the parquet equations as in the zero-dimensional case. We first note the following identities: $(f\circ g)=(\hat{f}\circ\hat{g})$, $\widehat{f\circ g}=f\circ\hat{g}=\hat{f}\circ g$, and $\widehat{f*g}(\mathbf{k})=\hat{f}(\mathbf{k})\hat{g}(\mathbf{k})$. Inserting $\Lambda_i(\mathbf{k})=\Gamma(\mathbf{k})-\Pi_i(\mathbf{k})$ into (3.6b) and (3.6c) and using $\hat{\Gamma}=\Gamma$ from (2.10), we obtain

$$\Pi_2(\mathbf{k})=\hat{\Pi}_3(\mathbf{k})=\frac{-2x\Gamma^2(\mathbf{k})}{1-2x\Gamma(\mathbf{k})}. \tag{3.9}$$

Now, inserting this into (3.6a),

$$\begin{aligned}\Pi_1(\mathbf{k})&=-x[(R+\Pi_2+\Pi_3)\circ\Gamma](\mathbf{k})\\&=-x[(R+2\Pi_2)\circ\Gamma](\mathbf{k}).\end{aligned} \tag{3.10}$$

Therefore, inserting (3.9) and (3.10) into (3.7), we obtain an equation for $\Gamma(\mathbf{k})$. In terms of the structure factor $\Delta(\mathbf{k})=1-2x\Gamma(\mathbf{k})$, this equation becomes

$$\frac{1-\Delta(\mathbf{k})}{\Delta(\mathbf{k})}=xR(\mathbf{k})+x(R\circ\Delta)(\mathbf{k})-\left(\left[\frac{(1-\Delta)^2}{\Delta}\right]\circ\Delta\right)(\mathbf{k}). \tag{3.11}$$

This is our main equation mentioned in Sec. I that completely describes the structure factor of 2D vortex liquid in the absence of disorder. Note that we have kept the totally

irreducible part $R(\mathbf{k})$ in a general form. We note that, although this is an *exact* relation in a very simple form, it has little advantage for finding numerical solutions[18] over the coupled parquet equations, (3.6), (3.7), and (3.8) or another version to be described below. We believe, however, that this equation might open a possibility in the future for a nonperturbative *analytic* investigation on the 2D vortex liquid.

When we consider the disordered case in the next section, it will be *necessary* to decompose $\Gamma(\mathbf{k})$ into $f_R(\mathbf{k})$ and $\hat{f}_R(\mathbf{k})$ using (2.10) and consider the parquet equation in terms of $f_R(\mathbf{k})$ arising from the faithful representation of Feynman diagrams as in Fig. 1. Equation (3.9) suggests the following decompositions:

$$\Pi_1(\mathbf{k})=\frac{1}{2}[\Gamma_1(\mathbf{k})+\hat{\Gamma}_1(\mathbf{k})],$$

$$\Pi_2(\mathbf{k})=\hat{\Pi}_3(\mathbf{k})=\frac{1}{2}[\Gamma_2(\mathbf{k})+\hat{\Gamma}_3(\mathbf{k})],$$

$$\Lambda_1(\mathbf{k})=\frac{1}{2}[I_1(\mathbf{k})+\hat{I}_1(\mathbf{k})],$$

$$\Lambda_2(\mathbf{k})=\hat{\Lambda}_3(\mathbf{k})=\frac{1}{2}[I_2(\mathbf{k})+\hat{I}_3(\mathbf{k})],$$

for some functions I_i and Γ_i. Inserting these into (3.6), we have

$$\Gamma_1(\mathbf{k})=-x(I_1\circ f_R)(\mathbf{k}), \tag{3.12a}$$

$$\Gamma_2(\mathbf{k})=-x[I_2(\mathbf{k})f_R(\mathbf{k})+I_2(\mathbf{k})\hat{f}_R(\mathbf{k})+\hat{I}_3(\mathbf{k})f_R(\mathbf{k})], \tag{3.12b}$$

$$\Gamma_3(\mathbf{k})=-x(I_3*f_R)(\mathbf{k}), \tag{3.12c}$$

and

$$f_R(\mathbf{k})=f_B(\mathbf{k})+\sum_{i=1}^{3}\Gamma_i(\mathbf{k}), \tag{3.12d}$$

$$I_i(\mathbf{k})=f_B(\mathbf{k})+\sum_{j\neq i}\Gamma_j(\mathbf{k}). \tag{3.12e}$$

This version of the parquet equations has been previously given in Ref. 5.

IV. PARQUET-GRAPH RESUMMATION: DISORDERED CASE

For the disordered case, one has to construct the parquet equation for the vertex function containing n-replica indices. Let us first consider the two-dimensional case directly. It is straightforward to generalize (3.6) to the present case. By putting the replica indices in the diagrams in Fig. 5, we have

$$\Pi^{(1)}_{ab,cd}(\mathbf{k})=-x\sum_{e,f}(\Lambda^{(1)}_{ab,ef}\circ\Gamma_{ef,cd})(\mathbf{k}), \tag{4.1a}$$

$$\Pi^{(2)}_{ab,cd}(\mathbf{k})=-2x\sum_{e,f}\Lambda^{(2)}_{ae,cf}(\mathbf{k})\Gamma_{fb,ed}(\mathbf{k}), \tag{4.1b}$$

$$\Pi^{(3)}_{ab,cd}(\mathbf{k})=-2x\sum_{e,f}(\Lambda^{(3)}_{ae,fd}*\Gamma_{fb,ce})(\mathbf{k}). \tag{4.1c}$$

The remaining equations follow from (3.7) and (3.8):

$$\Gamma_{ab,cd}(\mathbf{k})=R_{ab,cd}(\mathbf{k})+\sum_{i=1}^{3}\Pi^{(i)}_{ab,cd}(\mathbf{k}), \tag{4.1d}$$

$$\Lambda^{(i)}_{ab,cd}(\mathbf{k})=R_{ab,cd}(\mathbf{k})+\sum_{j\neq i}\Pi^{(j)}_{ab,cd}(\mathbf{k}), \tag{4.1e}$$

where

$$R_{ab,cd}(\mathbf{k})\simeq\Gamma^{(B)}_{ab,cd}(\mathbf{k})=\delta_{ac}\delta_{bd}(\delta_{ab}-\theta)\exp(-\mathbf{k}^2/2\mu^2)$$

in the parquet approximation.

As one can see from (2.10), in order to take the $n\to 0$ limit, one needs to decompose the above equations as in the previous section and to get equations analogous to (3.12). First, we note that

$$\hat{\Lambda}^{(3)}_{ab,dc}(\mathbf{k})=\Lambda^{(2)}_{ab,cd}(\mathbf{k}),\quad \hat{\Pi}^{(3)}_{ab,dc}(\mathbf{k})=\Pi^{(2)}_{ab,cd}(\mathbf{k}).$$

Therefore, we can write, for some functions Γ_i, Ξ_i, I_i, and J_i,

$$\Pi^{(1)}_{ab,cd}(\mathbf{k})=\frac{1}{2}\delta_{ac}\delta_{bd}[\delta_{ab}\Gamma_1(\mathbf{k})-\theta\Xi_1(\mathbf{k})]+\frac{1}{2}\delta_{ad}\delta_{bc}[\delta_{ab}\hat{\Gamma}_1(\mathbf{k})-\theta\hat{\Xi}_1(\mathbf{k})],$$

$$\Pi^{(2)}_{ab,cd}(\mathbf{k})=\hat{\Pi}^{(3)}_{ab,dc}(\mathbf{k})=\frac{1}{2}\delta_{ac}\delta_{bd}[\delta_{ab}\Gamma_2(\mathbf{k})-\theta\Xi_2(\mathbf{k})]+\frac{1}{2}\delta_{ad}\delta_{bc}[\delta_{ab}\hat{\Gamma}_3(\mathbf{k})-\theta\hat{\Xi}_3(\mathbf{k})],$$

and

$$\Lambda^{(1)}_{ab,cd}(\mathbf{k})=\frac{1}{2}\delta_{ac}\delta_{bd}[\delta_{ab}I_1(\mathbf{k})-\theta J_1(\mathbf{k})]+\frac{1}{2}\delta_{ad}\delta_{bc}[\delta_{ab}\hat{I}_1(\mathbf{k})-\theta\hat{J}_1(\mathbf{k})],$$

$$\Lambda^{(2)}_{ab,cd}(\mathbf{k})=\hat{\Lambda}^{(3)}_{ab,dc}(\mathbf{k})=\frac{1}{2}\delta_{ac}\delta_{bd}[\delta_{ab}I_2(\mathbf{k})-\theta J_2(\mathbf{k})]+\frac{1}{2}\delta_{ad}\delta_{bc}[\delta_{ab}\hat{I}_3(\mathbf{k})-\theta\hat{J}_3(\mathbf{k})].$$

Inserting these expressions and (2.10) into (4.1) and eliminating one term that contains an explicit factor of n, we get the following set of parquet equations in the presence of disorder:

$$\Gamma_1(\mathbf{k})=-x(I_1\circ f_R-\theta I_1\circ v_R-\theta J_1\circ f_R)(\mathbf{k}),$$

$$\Gamma_2(\mathbf{k}) = -x\{I_2(\mathbf{k})f_R(\mathbf{k}) + I_2(\mathbf{k})[\hat{f}_R(\mathbf{k}) - \theta\hat{v}_R(\mathbf{k})] + [\hat{I}_3(\mathbf{k}) - \theta\hat{J}_3(\mathbf{k})]f_R(\mathbf{k})\},$$

$$\Gamma_3(\mathbf{k}) = -x(I_3 * f_R - \theta I_3 * v_R - \theta J_3 * f_R)(\mathbf{k}),$$

and

$$\Xi_1(\mathbf{k}) = x\,\theta(J_1 \circ v_R)(\mathbf{k}),$$

$$\Xi_2(\mathbf{k}) = -x\{I_2(\mathbf{k})v_R(\mathbf{k}) + J_2(\mathbf{k})f_R(\mathbf{k}) + J_2(\mathbf{k})[\hat{f}_R(\mathbf{k}) - \theta\hat{v}_R(\mathbf{k})] + [\hat{I}_3(\mathbf{k}) - \theta\hat{J}_3(\mathbf{k})]v_R(\mathbf{k})\},$$

$$\Xi_3(\mathbf{k}) = x\,\theta(J_3 * v_R)(\mathbf{k})$$

with

$$f_R(\mathbf{k}) = f_B(\mathbf{k}) + \sum_{i=1}^{3} \Gamma_i(\mathbf{k}), \tag{4.2a}$$

$$v_R(\mathbf{k}) = v_B(\mathbf{k}) + \sum_{i=1}^{3} \Xi_i(\mathbf{k}), \tag{4.2b}$$

and

$$I_i(\mathbf{k}) = f_B(\mathbf{k}) + \sum_{j\neq i} \Gamma_j(\mathbf{k}), \tag{4.3a}$$

$$J_i(\mathbf{k}) = v_B(\mathbf{k}) + \sum_{j\neq i} \Xi_j(\mathbf{k}). \tag{4.3b}$$

Before solving these complicated equations, we consider first the zero-dimensional toy model where the parquet equations reduce to a set of algebraic equations as in (3.4).

$d = 0$

For $d = 0$, the partition function is again a simple integral,

$$Z(\alpha_H, \tau, \beta) = \int \frac{d\psi d\psi^*}{2\pi} \exp\left(-(\alpha_H + \tau)|\psi|^2 - \frac{\beta}{2}|\psi|^4\right) = \sqrt{\frac{\pi}{2\beta}}\,\mathrm{erfc}\left(\frac{\alpha_H + \tau}{\sqrt{2\beta}}\right)\exp\left(\frac{(\alpha_H + \tau)^2}{2\beta}\right).$$

Averaging over τ with respect to (2.2), we have

$$-\overline{\ln Z}(\sigma, \beta, \theta) = \frac{1}{2}\ln\beta - \sigma^2 - \frac{\theta}{2} - \frac{1}{\sqrt{\theta\pi}}\int_{-\infty}^{\infty} d\sigma' e^{-(\sigma-\sigma')^2/\theta} \ln \mathrm{erfc}(\sigma'), \tag{4.4}$$

where $\sigma = \alpha_H/\sqrt{2\beta}$, and $\theta = \lambda/\beta$ as before.

The quantities corresponding to $f_R(\mathbf{k})$ and $v_R(\mathbf{k})$ in the zero-dimensional case are defined by

$$f_R \equiv -\frac{\alpha_R^4}{2\beta}[\overline{\langle|\psi|^4\rangle} - 2\overline{\langle|\psi|^2\rangle^2}] = -\frac{\alpha_R^4}{\beta}\left[\frac{\partial}{\partial\beta} + \frac{\partial^2}{\partial\alpha_H^2}\right]\overline{\ln Z},$$

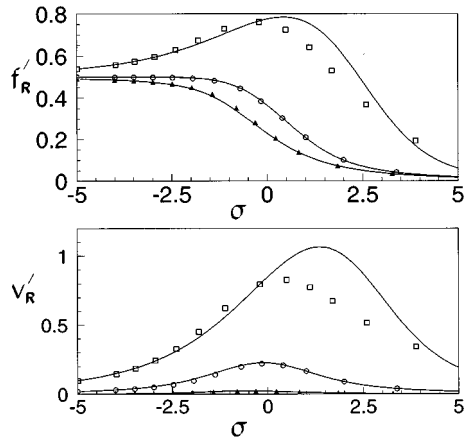

FIG. 7. The renormalized four-point vertex functions, f_R' and v_R' for the disordered zero-dimensional model as functions of temperature σ. The filled triangles, circles, and squares are obtained from the parquet approximation for $\theta = 0.1$, 1.0, and 5.0, respectively. The solid lines are the corresponding exact solutions.

$$v_R \equiv \frac{\alpha_R^4}{\beta}[\overline{\langle|\psi|^2\rangle^2} - [\overline{\langle|\psi|^2\rangle}]^2] = -\frac{\alpha_R^2}{\beta} - \frac{\alpha_R^4}{\beta}\left[2\frac{\partial}{\partial\beta} + \frac{\partial^2}{\partial\alpha_H^2}\right]\overline{\ln Z},$$

where $\alpha_R^{-1} \equiv \overline{\langle|\psi|^2\rangle} = -\partial\,\overline{\ln Z}/\partial\alpha_H$. These quantities can easily be evaluated as functions of σ and θ using (4.4).

On the other hand, the parquet equations for f_R and v_R take exactly the same form as (4.2), (4.3), if we make the following simplifications: the binary operations $\circ$ and $*$ become multiplications between two factors; the transformation $\hat{f}$ has no effect, $\hat{f} = f$; x is replaced by $\rho \equiv \beta/\alpha_R$; and finally $f_B = v_B = 1$. It is then straightforward to eliminate I_i (or Γ_i) and J_i (or Ξ_i) from the parquet equations in favor of $f_R' \equiv \rho f_R$ and $v_R' \equiv \rho v_R$. The parquet equations then reduce to the following coupled algebraic equations:

$$\frac{2f_R'}{(1 - f_R' + v_R')(1 + v_R')} + \frac{f_R'}{(1 - f_R' + v_R')(1 - 2f_R' + v_R')} - 2f_R' = \rho, \tag{4.5}$$

$$\frac{2v_R'}{1 + v_R'} + \frac{v_R'}{(1 - 2f_R' + v_R')^2} - 2v_R' = \theta\rho. \tag{4.6}$$

For given θ and ρ, one can find the corresponding solutions f_R' and v_R' to these equations. We can then use the Dyson equation (2.13),

$$\sigma = \frac{1}{\sqrt{2\rho}}\{1 - \rho(2 - \theta) + \rho[2(f_R' - v_R') - \theta(2f_R' - v_R')]\}$$

to find a relation between ρ and σ: $\rho = \rho(\sigma)$ for given θ. Using this, we obtain $f_R'(\sigma)$ and $v_R'(\sigma)$ for given θ. These are shown in Fig. 7 together with the exact solutions. For

$\theta \lesssim 1$, the parquet results show excellent agreement with the exact solutions. As θ becomes larger, however, the discrepancies between two solutions grow. This analysis for the zero-dimensional model suggests that the parquet approximation is in general very good when the strength of disorder is moderate. But, the diagrams omitted in the parquet approximation might produce quantitative errors in the strong disorder regime. We note, however, that physical quantities in this approximation remain smooth as functions of θ unlike other approximation methods[19] on this system.

V. RESULTS AND ANALYSIS

For the case of the two-dimensional system, one has to solve a set of coupled integral equations for $f_R(\mathbf{k})$ and $v_R(\mathbf{k})$, (4.2) and (4.3), containing two parameters x and θ. We consider a rotationally symmetric case where all vertex functions depend only on $K \equiv |\mathbf{k}|/\mu$. We apply a similar numerical technique to the one used in Ref. 5. In practice, we find it convenient to work with $h_R(K) \equiv f_R(K) - \theta v_R(K)$ and $v_R(K)$. For a given set of irreducible parts, $\{I_i(K)\}$ and $\{J_i(K)\}$, Eqs. (4.2) are coupled *linear* integral equations for h_R and v_R. We first solve these equations for h_R for fixed v_R by numerically inverting a matrix,[20] and then solve for v_R using the solution h_R. We then update the irreducible parts using (4.3). The solution to the parquet equations is obtained by iterating this procedure.

A fast convergence can be obtained if we choose the initial functions, $\{I_i\}$, $\{J_i\}$, and v_R close to the actual solutions. At high enough temperatures, it is sufficient to start from $I_i = J_i = v_R = \exp(-K^2/2)$. As one goes into the low-temperature regime, it is necessary to use the solution at a temperature close to the desired temperature as initial functions. We face the same numerical difficulty as in Ref. 5 as the temperature is lowered, namely, one has to use a finer mesh in K space as well as a larger cutoff in order to get a low-temperature solution. In this case, we have a *coupled* set of equations, which requires an additional computing time. The minimum temperature we used was $\alpha_T \simeq -8.5$ where the cutoff was at $K = 15$ and the number of mesh points was 600. We also find it difficult to solve the parquet equations directly for arbitrarily large values of θ. Again, one needs to start from the actual solution for θ close to the value for which the structure factor is to be calculated. In the present analysis, we were able to obtain $\Delta(K)$ for three values of θ; $\theta = 0.1$, 0.2, and 0.3.

In Fig. 8, we first present the renormalized propagator $\sqrt{x} \sim \alpha_R^{-1}$ as a function of temperature α_T for three values of θ. Compared to the pure ($\theta = 0$) case, $\alpha_T(x)$ as a function of x shows very little deviation. In general, one finds that the same value of parameter x represents a slightly higher temperature as θ increases.

In Figs. 9 and 10, the structure factor is plotted for various values of α_T and θ. The structure factor develops a collection of peaks around the reciprocal-lattice vectors (RLV) of the triangular lattice. As the temperature is lowered for fixed θ, one can clearly see from Fig. 9 that the first peak grows with decreasing width. This can be interpreted as a growing short-range translational order in the disordered vortex liquid. The length scale R_c over which this order exists can be obtained from the inverse width of the first peak, or equivalently from the peak height.[5,9] For fixed temperatures, we find that the length scale decreases as the strength of disorder increases (see Fig. 10). The result is consistent with an intuitive picture where the disorder prevents ordering on long length scales. In Fig. 11, we show the height of the first peak as a function of temperature for $\theta = 0.1$, 0.2, and 0.3. We find that the length scale R_c grows as $|\alpha_T|$ with decreasing proportionality constant for increasing θ. We recall that, in the absence of disorder, the length scale characterizing a growing crystalline order also grows as $|\alpha_T|$. But, from Fig. 11, we find that the rate of this growth gets smaller as the disorder gets stronger. In the next subsection, we show that one can derive this behavior analytically from the parquet equations.

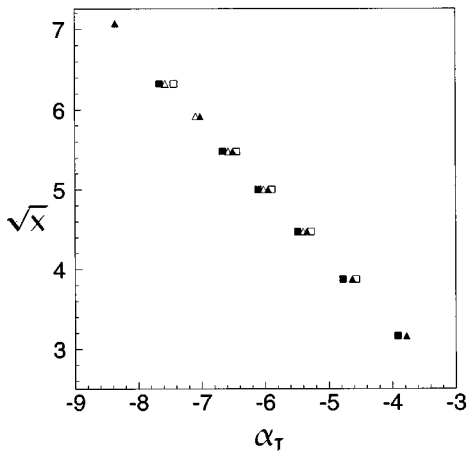

FIG. 8. The renormalized propagator ($\mu^2/2\pi\alpha_R \sim \sqrt{x}$) as a function of temperature α_T in $d = 2$. The filled squares are obtained from the parquet approximation in the pure case. The open triangles, filled triangles, and open squares correspond to the parquet approximation for $\theta = 0.1$, 0.2, and 0.3, respectively.

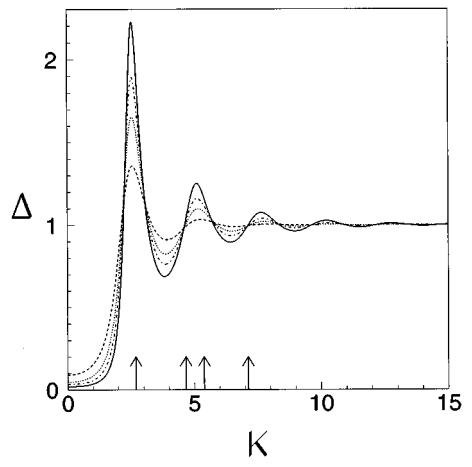

FIG. 9. The structure factor for fixed $\theta = 0.2$ and for various temperatures (dashed line: $\alpha_T = -3.78$, dotted line: $\alpha_T = -5.34$, dot-dashed line: $\alpha_T = -6.51$, and solid line: $\alpha_T = -8.36$). The arrows indicate the positions of RLV of the triangular lattice. Since the second and the third RLV are closely spaced, our solution could not resolve these peaks.

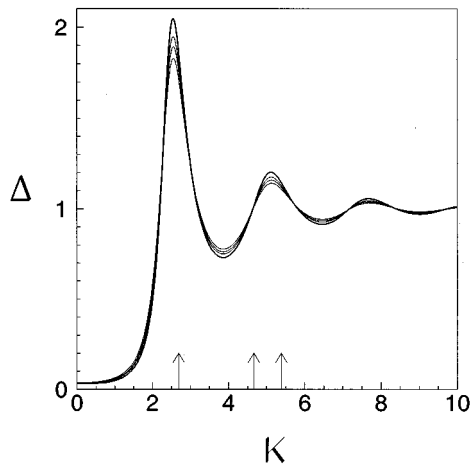

FIG. 10. The structure factor for fixed $x=30$ (or slightly varying α_T; $-6.67<\alpha_T<-6.45$), and for various values of θ: $\theta=0$ (thick line), 0.1, 0.2, and 0.3. The peaks are getting smaller as the strength of disorder (θ) increases.

Parquet equations for $\theta \ll 1$

For very weak disorder, $\theta \ll 1$, one can extract from the parquet equations the small-θ behavior of the structure factor $\Delta(\mathbf{k})$ around the pure ($\theta=0$) solution. One can in fact derive the temperature dependence of the length scale R_c for small θ from the parquet equations. In order to do that, we need to find the parquet equation analogous to (3.6), (3.7), and (3.8) for $\Gamma(\mathbf{k})=(1/2)[h_R(\mathbf{k})+\hat{h}_R(\mathbf{k})]$. Out of the functions used in (4.2) and (4.3), we define

$$\Lambda_1(\mathbf{k}) \equiv \frac{1}{2}[I_1(\mathbf{k})+\hat{I}_1(\mathbf{k})-\theta(J_1(\mathbf{k})+\hat{J}_1(\mathbf{k}))],$$

$$\Lambda_2(\mathbf{k}) \equiv \frac{1}{2}[I_2(\mathbf{k})+\hat{I}_3(\mathbf{k})-\theta(J_2(\mathbf{k})+\hat{J}_3(\mathbf{k}))],$$

$$\Lambda_3(\mathbf{k}) \equiv \hat{\Lambda}_2(\mathbf{k})$$

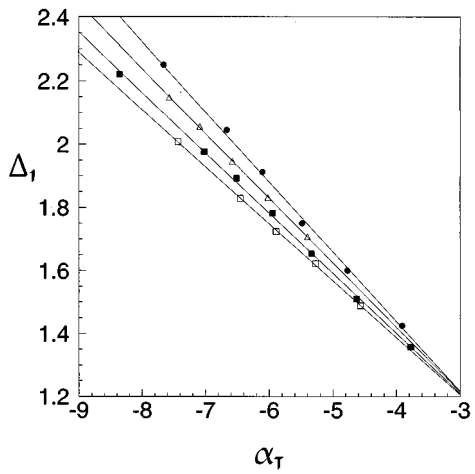

FIG. 11. The height Δ_1 of the first peak as a function of temperature. The filled circles, triangles, filled squares, and open squares correspond to the solutions at $\theta=0$, 0.1, 0.2, and 0.3, respectively. The solid lines are linear fits.

and

$$\Pi_1(\mathbf{k}) \equiv \frac{1}{2}[\Gamma_1(\mathbf{k})+\hat{\Gamma}_1(\mathbf{k})-\theta(\Xi_1(\mathbf{k})+\hat{\Xi}_1(\mathbf{k}))],$$

$$\Pi_2(\mathbf{k}) \equiv \frac{1}{2}[\Gamma_2(\mathbf{k})+\hat{\Gamma}_3(\mathbf{k})-\theta(\Xi_2(\mathbf{k})+\hat{\Xi}_3(\mathbf{k}))],$$

$$\Pi_3(\mathbf{k}) \equiv \hat{\Pi}_2(\mathbf{k}).$$

Using these functions and the original parquet equations, (4.2) and (4.3), one can find a set of equations for $\Gamma(\mathbf{k})$ as follows:

$$\Gamma(\mathbf{k}) = \Gamma_B(\mathbf{k}) + \sum_{i=1}^{3} \Pi_i(\mathbf{k}), \tag{5.1a}$$

$$\Lambda_i(\mathbf{k}) = \Gamma(\mathbf{k}) - \Pi_i(\mathbf{k}), \tag{5.1b}$$

$$\Pi_1(\mathbf{k}) = -x(\Lambda \circ \Gamma)(\mathbf{k}), \tag{5.1c}$$

$$\Pi_2(\mathbf{k}) = -2x\left[\Lambda_2(\mathbf{k})\Gamma(\mathbf{k}) - \frac{\theta^2}{4}J_2(\mathbf{k})v_R(\mathbf{k})\right], \tag{5.1d}$$

$$\Pi_3(\mathbf{k}) = \hat{\Pi}_2(\mathbf{k}), \tag{5.1e}$$

where

$$\Gamma_B(\mathbf{k}) = (1-\theta)\exp(-\mathbf{k}^2/2\mu^2), \tag{5.2}$$

and we have used the above-mentioned identities involving the binary operations, $\circ$ and *. Note that these equations are almost the same as those given in the pure case, (3.6), (3.7), and (3.8). One extra term in (5.1d) comes from the subtraction of the diagram containing an explicit factor of n. There is of course the second equation for v_R, which couples nontrivially to these equations.

Note that the structure factor $\Delta(\mathbf{k})$ is just given by $\Delta=1-2x\Gamma$, and we can simplify the above equations as done in the pure case to get one equation for the structure factor. From (5.1d) and the J_2 equation in (4.3b), we have

$$J_2(\mathbf{k}) = v_R(\mathbf{k})\frac{1+2x\Lambda_2(\mathbf{k})}{\Delta(\mathbf{k})-2\theta x v_R(\mathbf{k})}.$$

Inserting this into (5.1d), we obtain

$$\Lambda_2(\mathbf{k}) = \frac{1}{2x}\left[-1+\frac{\Delta(\mathbf{k})-2\theta x v_R(\mathbf{k})}{[\Delta(\mathbf{k})-\theta x v_R(\mathbf{k})]^2}\right].$$

Now using (5.1a) and the identities mentioned above, we find

$$\frac{\Delta(\mathbf{k})-2\theta x v_R(\mathbf{k})}{[\Delta(\mathbf{k})-\theta x v_R(\mathbf{k})]^2} = 1 + x\Gamma_B(\mathbf{k}) + x(\Gamma_B \circ \Delta)(\mathbf{k}) - \left(\left[\Delta - 2 + \frac{\Delta - 2\theta x v_R}{[\Delta-\theta x v_R]^2}\right]\circ\Delta\right)(\mathbf{k}). \tag{5.3}$$

When $\theta=0$, this reduces to (3.11). So far we have not made any assumptions on the magnitude of θ. For small θ, one may consider the lowest-order perturbation in the structure

factor as compared to the pure solution. Note that, up to $O(\theta)$, the equation takes the same form as in the $\theta=0$ case, except that $\Gamma_B(\mathbf{k})$ in (5.2) contains an additional factor of $(1-\theta)$. This means that for $\theta \ll 1$, the solution for given θ and x is the same as the pure solution, denoted by Δ_0, at $x(1-\theta)$,

$$\Delta(\mathbf{k};x,\theta) \simeq \Delta_0[\mathbf{k};x(1-\theta)], \quad \theta \ll 1. \tag{5.4}$$

For given x and θ, α_T is determined via (2.13). If we denote by $\alpha_T^0(x)$ the relation between α_T and x for $\theta=0$, then from (2.13) and (5.4) we deduce that to $O(\theta)$

$$\alpha_T(x) \simeq \alpha_T^0[x(1-\theta)] - \frac{\theta}{2}[2\sqrt{x} + \alpha_T^0(x)]. \tag{5.5}$$

We note that, for $\theta=0$, $\alpha_T^0(x)=[1-x\beta_A(x)]/\sqrt{x} \sim -\sqrt{x}\beta_A$ as $\alpha_T \to -\infty$, where the generalized Abrikosov ratio changes from 2 at high temperatures to some low-temperature limit, β_A. In the pure case, we found[5] that the length scale grows as $\sim|\alpha_T^0(x)| \sim \sqrt{x}\beta_A(x)$. Using (5.4) and (5.5), one can derive that

$$R_c \sim \beta_A\sqrt{(1-\theta)x} \sim \left[1-\theta\left(\frac{1}{2}+\frac{1}{\beta_A}\right)\right]|\alpha_T| \tag{5.6}$$

as $\alpha_T \to -\infty$. As mentioned before, this behavior is already captured in our numerical solution (see Fig. 11).

VI. GENERALIZATION TO THREE DIMENSIONS

In this section, we apply the parquet resummation method to a three-dimensional vortex liquid system. We shall demonstrate that, while the generalization of the parquet equations to three dimensions is straightforward, it is virtually impossible to solve the equations using the same numerical technique as in the 2D case. We shall then discuss a possible analytic approach to the problem.

We consider only the pure case for simplicity. The order parameter $\Psi(x,y,r_\perp)$ in 3D depends on the coordinate $r_\perp$ perpendicular to the (x,y) plane. In the lowest-Landau-level approximation, the order parameter takes the form

$$\Psi(x,y,r_\perp) = \phi(z,r_\perp)\exp\left(-\frac{\mu^2}{4}|z|^2\right).$$

The GL free energy analogous to (2.3) is given by

$$F[\phi] = \int dr_\perp dz^* dz \left((|\partial_\perp \phi|^2 + \alpha_H|\phi|^2)e^{-\mu^2|z|^2/2} + \frac{\beta}{2}\exp(-\mu^2|z|^2)|\phi(z,r_\perp)|^4 \right),$$

where $\partial_\perp = \partial/\partial r_\perp$. The renormalized propagator can be written as

$$G(\zeta^*,z;q) = \frac{\mu^2}{2\pi}\mathcal{G}(q)\exp\left(\frac{\mu^2}{2}\zeta^* z\right), \tag{6.1}$$

where q is the Fourier momentum corresponding to $r_\perp$. For the bare propagator, $\mathcal{G}_0(q)=(q^2+\alpha_H)^{-1}$. But, the renormalization drives $\mathcal{G}(q)$ into a general function. This is in contrast to the two-dimensional case where the propagator is completely described by one parameter α_R.

Similarly, the renormalized four-point vertex carries four momenta, q_1, q_2, q_3, and q_4, in addition to $\mathbf{k}$ describing the correlation in the (x,y) plane. Among the four momenta only three will be independent due to the momentum conservation $(q_1+q_2=q_3+q_4)$. Using, for example, new variables, $s \equiv q_1+q_2$, $t \equiv q_1-q_3$, and $u \equiv q_1-q_4$, one can describe the renormalized four-point vertex function in terms of $\Gamma(s,t,u;\mathbf{k})$. The parquet equations for Γ follow from Fig. 5. By evaluating the diagrams in Fig. 5 using the momentum conservation on each vertex, one finds that

$$\Pi_1(s,t,u;\mathbf{k}) = -\eta\int\frac{dq}{2\pi}\Omega(q,s)\left[\Lambda_1\left(s,\frac{s+t+u}{2}-q,q-\frac{s-t-u}{2}\right)\circ\Gamma\left(s,q-\frac{s-t+u}{2},q-\frac{s+t-u}{2}\right)\right](\mathbf{k}),$$

$$\Pi_2(s,t,u;\mathbf{k}) = -2\eta\int\frac{dq}{2\pi}\Omega(q,t)\Lambda_2\left(q+\frac{s-t+u}{2},t,\frac{s+t+u}{2}-q;\mathbf{k}\right)\Gamma\left(q+\frac{s-t-u}{2},t,q-\frac{s+t-u}{2};\mathbf{k}\right),$$

$$\Pi_3(s,t,u;\mathbf{k}) = -2\eta\int\frac{dq}{2\pi}\Omega(q,u)\left[\Lambda_3\left(q+\frac{s+t-u}{2},\frac{s+t+u}{2}-q,u\right)*\Gamma\left(q+\frac{s-t-u}{2},q-\frac{s-t+u}{2},u\right)\right](\mathbf{k}),$$

where $\eta \equiv \beta\mu^2/2\pi$ and $\Omega(q,q') \equiv \mathcal{G}(q)\mathcal{G}(q-q')$ and $\circ$ and $*$ operate on the two-dimensional momentum $\mathbf{k}$ as before. The remaining parquet equations take the same form as in the 2D case:

$$\Gamma(s,t,u;\mathbf{k}) = R(s,t,u;\mathbf{k}) + \sum_{i=1}^{3}\Pi_i(s,t,u;\mathbf{k}),$$

$$\Lambda_i(s,t,u;\mathbf{k}) = \Gamma(s,t,u;\mathbf{k}) - \Pi_i(s,t,u;\mathbf{k}),$$

where R accounts for the totally irreducible parts, which is set to

$$R(s,t,u;\mathbf{k}) \simeq \exp(-\mathbf{k}^2/2\mu^2)$$

independent of s,t,u in the parquet approximation.

The first difficulty one faces when one tries to solve the above parquet equations as in the 2D case is the fact that the propagator is given as an unknown *function* in this case. In the 2D problem, we were able to determine the unknown

constant α_R (or x) self-consistently using the Dyson equation. In this case, we have a functional self-consistent equation for the self-energy $\Sigma(q)=\mathcal{G}^{-1}(q)-\mathcal{G}_0^{-1}(q)$ as follows:

$$\Sigma(q)=2\eta\int\frac{dq'}{2\pi}\mathcal{G}(q')$$
$$-2\eta^2\frac{2\pi}{\mu^2}\int\frac{d^2\mathbf{k}}{(2\pi)^2}\frac{dq'dq''}{(2\pi)^2}e^{-\mathbf{k}^2/2\mu^2}\mathcal{G}(q')\mathcal{G}(q'')\mathcal{G}(q$$
$$+q'-q'')\Gamma(q+q',q-q'',q''-q';\mathbf{k}).$$

Even if one uses this self-consistent relation, the parquet equations are coupled integral equations for the function Γ of four independent variables (s,t,u and $|\mathbf{k}|$). Storing all the data for Γ and for all the irreducible parts, Λ_i in the numerical calculation will be a formidable task. Furthermore, the integrations in the equations become multiple sums and therefore the previous numerical method of inverting a matrix becomes more cumbersome. One may have to resort to a direct iteration, which converges slower than the numerical inversion of matrices.

These numerical difficulties, however, should not discourage one from attempting to get some nonperturbative information from the parquet equations. In 2D, the parquet equations seem to be a minimal set of equations that predicts the growing translational order in the (x,y) plane, whose length scale is characterized by R_c. Thus, we expect that the above 3D parquet equations contain among other things nonperturbative information on various length scales characterizing the low-temperature regime of the system. In addition to R_c, the 3D system may have growing length scales for the correlation in the $r_\perp$ direction. We denote by ξ_L the length scale arising from the propagator $\mathcal{G}$ and by L_c the one associated with the 3D structure factor $S(\mathbf{k},q)\equiv(2\pi/\mu^2)\exp(\mathbf{k}^2/2\mu^2)\tilde{\chi}(\mathbf{k},q)$ [see (2.4)], where

$$S(\mathbf{k},q)=\int\frac{dq'}{2\pi}\mathcal{G}(q')\mathcal{G}(q+q')$$
$$-2\eta\int\frac{dq'dq''}{(2\pi)^2}\mathcal{G}(q')\mathcal{G}(q'')\mathcal{G}(q+q')\mathcal{G}(q$$
$$+q'')\Gamma(q+q'+q'',q,q'-q'';\mathbf{k}).$$

If one uses in the parquet equations some kinds of low-temperature asymptotic forms for $\mathcal{G}(q)$ and $S(\mathbf{k},q)$ which are characterized by the length scales, ξ_L, L_c, and R_c, one might be able to extract nonperturbative relations for these length scales and the temperature. We have tried a simple ansatz where $\mathcal{G}$ and S are represented as δ-function-like sharp peaks around $q=0$ and $\mathbf{k}=\mathbf{G}$ (RLV). The length scales are set to be equal to the inverse width of the corresponding peaks. But, we found that these forms are too simplified to produce a sufficient amount of information on the temperature dependences of each length scale. We believe that more sophisticated asymptotic forms are needed for the analysis of the 3D parquet equations. This point will be discussed again in the next section.

VII. DISCUSSION AND SUMMARY

In this paper, we applied the parquet resummation method to the 2D vortex liquid with and without quenched impurities and to the 3D vortex liquid in the absence of disorder. In the 2D system, we were able to solve the parquet equations numerically and find the length scale R_c. The temperature dependence of R_c was also obtained. In the pure 2D vortex liquid, we found in the previous paper[5] that the asymptotic forms, $\Delta(\mathbf{k})\sim 2\pi\mu^2\Sigma_{\mathbf{G}\neq\mathbf{0}}\delta^{(2)}(\mathbf{k}-\mathbf{G})$, or equivalently $f_R(\mathbf{k})\sim x^{-1}[1-\pi\mu^2\Sigma_{\mathbf{G}}\delta^{(2)}(\mathbf{k}-\mathbf{G})]$ solves the parquet equations if the inverse width of the δ-function peaks, or the length scale R_c behaves like $\sqrt{x}\sim|\alpha_T|$ as $\alpha_T\rightarrow-\infty$. In the disordered case, one can obtain similar low-temperature asymptotic forms for $f_R(\mathbf{k})$ and $v_R(\mathbf{k})$ in terms of δ functions around $\mathbf{k}\sim\mathbf{G}$. One can then obtain expressions for R_c similar to (5.6). These simple asymptotic forms, however, have some limitations. First of all, the amplitude of each δ-function peak cannot be determined from the parquet equations. It is also not clear whether one can use these representations in the strong disorder regime. In the previous section, we argued that an ansatz like $S(\mathbf{k},q)\sim\delta(q)\Sigma_{\mathbf{G}\neq\mathbf{0}}\delta^{(2)}(\mathbf{k}-\mathbf{G})$ was not enough to produce any useful nonperturbative information for the three-dimensional solution. We believe that finding appropriate low-temperature asymptotic forms for the vertex functions is a first step towards a more fruitful use of the parquet equations. To this end, a simple equation like (3.11) might be useful.

The effect of random impurities on the mixed state of a type-II superconductor is usually described by the so-called Larkin-Ovchinnikov argument,[4] which states that for a dimension $d<4$ the long-range crystalline order of the mixed state is destroyed by a weak disorder. For thin films ($d=2$), one can estimate the Larkin length scale R_c over which a short-range order persists as[4] $R_c\sim|\alpha_T|/\lambda$. Although the $|\alpha_T|$ dependence of R_c is the same as the present result, we note that there is a basic difference between our result and the LO-type argument. Since the LO argument starts from a perfect crystalline state where $\lambda=0, R_c=\infty$, a very small amount of disorder makes an abrupt change as can be seen from the $1/\sqrt{\lambda}$ dependence of R_c. Within the parquet approximation, there is no 2D crystalline phase and the pure system has a finite R_c at any finite temperature. As we have seen in the previous sections, the effect of small disorder is represented as a smooth decrease of this length scale.

In this paper, we have concentrated on a rotationally symmetric liquid state where the vertex functions depend only on the magnitude of $\mathbf{k}$. But, for example, in the presence of magnetoelastic interactions between vortices, one must consider general $\mathbf{k}$-dependent vertex functions in the parquet equations. We recall that the input parameters of the parquet equations are the temperature and the bare vertex functions, f_B and v_B. It would be interesting to study a situation where the bare vertex functions possess a nontrivial $\mathbf{k}$ dependence.

One could also generalize the present parquet resummation technique to study the dynamics of type-II superconductors. We expect that the parquet equations for the time-dependent Ginzburg-Landau theory can be obtained without much difficulty. But, the vertex functions will depend on the frequency as well as the usual momenta. Thus, one faces similar numerical difficulty to the 3D case. In addition, one

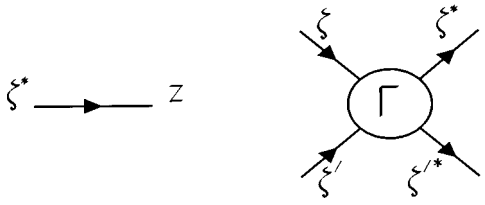

FIG. 12. Diagrammatic representation of the propagator and the four-point vertex.

has to be careful in taking the LLL limit.[22]

ACKNOWLEDGMENTS

We would like to thank T. Blum, A. J. Bray, M. J. W. Dodgson, and T. J. Newman for useful discussions.

APPENDIX: EVALUATION OF DIAGRAMS

Here we give some examples of evaluating the Feynman diagrams involved in the present work. Similar analysis can be found in the Appendix of Ref. 21. We consider only the pure case ($\lambda=0$) for simplicity. The results can easily be generalized to the disordered case carrying the replica indices. Feynman diagrams are constructed by connecting the propagator lines represented by (2.6) with the quartic vertices, which can be obtained from (2.7) as (see Fig. 12)

$$-\frac{\beta}{2}e^{-\mu^2(|\zeta|^2+|\zeta'|^2)/2}\int\frac{dkdk^*}{(2\pi)^2}\Gamma(\mathbf{k})e^{|k|^2/2\mu^2}\times\exp\left[-\frac{i}{2}[k^*(\zeta-\zeta')+(\zeta^*-\zeta'^*)k]\right].$$

By joining four propagator lines (starting from z_1^* and z_2^* and ending at z_3 and z_4) with this vertex, we have

$$-4\left(\frac{\beta}{2}\right)\left(\frac{\mu^2}{2\pi}\right)^4\frac{1}{\alpha_R^4}\int\frac{dkdk^*}{(2\pi)^2}\Gamma(\mathbf{k})e^{|k|^2/2\mu^2}\times\int\prod_{i=1}^{2}d\zeta_i d\zeta_i^* e^{-\mu^2(|\zeta_1|^2+|\zeta_2|^2)/2}\times\exp\left[\frac{\mu^2}{2}[z_1^*\zeta_1+z_2^*\zeta_2+\zeta_1^*z_3+\zeta_2^*z_4]-\frac{i}{2}[k^*(\zeta_1-\zeta_2)+(\zeta_1^*-\zeta_2^*)k]\right].$$

After performing the Gaussian integrals using

$$\int\prod_{i=1}^{m}d\zeta_i d\zeta_i^*\exp[-\mu^2(\zeta_i^*M_{ij}\zeta_j-a_i^*\zeta_i-\zeta_i^*b_i)]=\left(\frac{\pi}{\mu^2}\right)^m(\det M)^{-1}\exp[\mu^2(a_i^*M_{ij}^{-1}b_j)],\qquad\text{(A1)}$$

one obtains (2.9).

Let us evaluate the one-loop diagrams and derive (3.6). We consider only the first diagram of Fig. 5 and thus derive (3.6a). The remaining two diagrams can be evaluated in the same manner. The first one-loop diagram gives

$$8\left(\frac{\beta}{2}\right)^2\left(\frac{\mu^2}{2\pi}\right)^6\frac{1}{\alpha_R^6}\int\prod_{i=1}^{2}\frac{dk_i dk_i^*}{(2\pi)^4}\Lambda_1(\mathbf{k_1})\Gamma(\mathbf{k_2})\times e^{(|k_1|^2+|k_2|^2)/2\mu^2}\int\prod_{j=1}^{4}d\zeta_j d\zeta_j^*\exp\left(-\frac{\mu^2}{2}\sum_{j=1}^{4}\left|\zeta_j\right|^2\right)\times\exp\left[\frac{\mu^2}{2}(z_1^*\zeta_1+z_2^*\zeta_2+\zeta_3^*z_3+\zeta_4^*z_4+\zeta_1^*\zeta_3+\zeta_2^*\zeta_4)\right]\times\exp\left[-\frac{i}{2}[k_1^*(\zeta_1-\zeta_2)+(\zeta_1^*-\zeta_2^*)k_1+k_2^*(\zeta_3-\zeta_4)+(\zeta_3^*-\zeta_4^*)k_2]\right].$$

Integrating over ζ_i and ζ_i^* using (A.1) and changing the variables $\mathbf{k}_1+\mathbf{k}_2\to\mathbf{k}$, and $\mathbf{k}_1\to\mathbf{p}$, we obtain

$$8\left(\frac{\beta}{2}\right)^2\left(\frac{\mu^2}{2\pi}\right)^2\frac{1}{\alpha_R^6}e^{\mu^2(z_1^*z_3+z_2^*z_4)/2}\int\frac{dkdk^*dpdp^*}{(2\pi)^4}\Lambda_1(\mathbf{p})\times\Gamma(\mathbf{k}-\mathbf{p})e^{-|k|^2/2\mu^2}\exp\left[-\frac{i}{2}[k^*(z_3-z_4)+(z_1^*-z_2^*)k]+\frac{1}{2\mu^2}(k^*p-p^*k)\right].$$

Comparing this with the general expression (2.9), we find that the one-loop contribution from this diagram to the vertex function is

$$-\frac{\beta\mu^2}{2\pi\alpha_R^2}\int\frac{dpdp^*}{(2\pi)^2}\Lambda_1(\mathbf{p})\Gamma(\mathbf{k}-\mathbf{p})\exp\left(\frac{1}{2\mu^2}(k^*p-p^*k)\right),$$

which is equal to the right-hand side of (3.6a).

[1] A. A. Abrikosov, Zh. Éksp. Teor. Fiz. **32**, 1442 (1957) [Sov. Phys. JETP **5**, 1174 (1957)].
[2] M. P. A. Fisher, Phys. Rev. Lett. **62**, 1415 (1989); D. S. Fisher, M. P. A. Fisher, and D. A. Huse, Phys. Rev. B **43**, 130 (1991).
[3] D. R. Nelson and V. M. Vinokur, Phys. Rev. Lett. **68**, 2398 (1992); Phys. Rev. B **48**, 13 060 (1993).
[4] A. I. Larkin, Zh. Éksp. Teor. Fiz. **58**, 1466 (1970) [Sov. Phys. JETP **31**, 784 (1970)]; A. I. Larkin and Yu. N. Ovchinnikov, J. Low Temp. Phys. **34**, 409 (1979).
[5] J. Yeo and M. A. Moore, Phys. Rev. Lett. **76**, 1142 (1996).
[6] The parquet-graph resummation method has been widely applied to many areas of many-body physics. See, for example, I. T. Diatlov, V. V. Sudakov, and K. A. Ter-Martirosian, Zh. Éksp. Teor. Fiz. **32**, 767 (1957) [Sov. Phys. JETP **5**, 631 (1957)]; Yu. A. Bychkov, L. D. Gor'kov, and I. E. Dzyaloshinskii, *ibid.* **50**, 738 (1966); B. Roulet, J. Gavoret, and P. Nozières, Phys. Rev.

178, 1072 (1969); A. D. Jackson, A. Landeand, and R. A. Smith, Phys. Rep. **86**, 55 (1982); H. W. He and R. A. Smith, *ibid.* **223**, 227 (1992). It has also been used to describe critical phenomena; A. I. Larkin and D. E. Khmel'nitskii, Zh. Éksp. Teor. Fiz. **58**, 1466 (1970) [Sov. Phys. JETP **31**, 784 (1970)]; T. Tsuneto and E. Abrahams, Phys. Rev. Lett. **30**, 217 (1973); E. Abrahams and T. Tsuneto, Phys. Rev. B **11**, 4498 (1975); N. E. Bickers and D. J. Scalapino, *ibid.* **46**, 8050 (1992). Recently, a similar formalism to the one presented in this paper was used in a different physical context; P. Kleinert and H. Schlegel, Physica A **218**, 507 (1995).

[7] T. Natterman, Phys. Rev. Lett. **64**, 2454 (1990); T. Giamarchi and P. Le Doussal, *ibid.* **72**, 1530 (1994); **74**, 606 (1995).

[8] Z. Tešanović and L. Xing, Phys. Rev. Lett. **67**, 2729 (1991); Y. Kato and N. Nagaosa, Phys. Rev. B **47**, 2932 (1993); J. Hu and A. H. MacDonald, Phys. Rev. Lett. **71**, 432 (1993); R. Šášik and D. Stroud, Phys. Rev. B **49**, 16 074 (1994).

[9] J. A. O'Neill and M. A. Moore, Phys. Rev. B **48**, 374 (1993); M. J. W. Dodgson and M. A. Moore (unpublished).

[10] A. V. Nikulov, D. Y. Remisov, and V. A. Oboznov, Phys. Rev. Lett. **75**, 2586 (1995).

[11] E. Zeldov *et al.*, Nature (London) **375**, 373 (1995).

[12] D. E. Farrell *et al.* (unpublished).

[13] E. Brézin, D. R. Nelson, and A. Thiaville, Phys. Rev. B **31**, 7124 (1985).

[14] M. A. Moore and T. J. Newman, Phys. Rev. Lett. **75**, 533 (1995).

[15] In this paper, we assume that all the vertex functions have a reflection symmetry; e.g., $f_R(-\mathbf{k})=f_R(\mathbf{k})$ so that the exponential in the definition of $\hat{f}_R$ can be replaced by a cosine. This is certainly true for the liquid state where the system has a rotational symmetry and also true for a possible crystalline state having, for example, a triangular lattice structure. In this work, we consider only the liquid state, but the equations presented here are valid for a general case with a reflection symmetry.

[16] G. J. Ruggeri and D. J. Thouless, J. Phys. F **6**, 2063 (1976); R. Ikeda, T. Ohmi, and T. Tsuneto, J. Phys. Soc. Jpn. **59**, 1397 (1990); E. Brézin, A. Fujita, and S. Hikami, Phys. Rev. Lett. **65**, 1949 (1990); S. Hikami, A. Fujita, and A. I. Larkin, Phys. Rev. B **44**, 10 400 (1991); A. Fujita, S. Hikami, and A. I. Larkin, Physica C. **185-189**, 1883 (1991).

[17] The value of the parameter x is twice the one used in Refs. 16 and 5.

[18] The numerical difficulty is mainly due to the presence of Δ in the denominators of the equation. If one tries to solve the equation iteratively, the procedure becomes too sensitive to the region where $\Delta \simeq 0$.

[19] A. J. Bray, T. McCarthy, M. A. Moore, J. D. Reger, and A. P. Young, Phys. Rev. B **36**, 2212 (1987).

[20] W. H. Press *et al.*, *Numerical Recipes* (Cambridge University Press, Cambridge, 1992), p. 782.

[21] T. J. Newman and M. A. Moore (unpublished).

[22] T. Blum and M. A. Moore (unpublished).